Pergamon

Int. J. Solids Structures Vol. 35, Nos 28–29, pp. 3615–3634, 1998

0020–7683/98 $19.00 + .00

PII: S0020–7683(97)00228–X

PERIODIC CRACKING OF ELASTIC COATINGS

GARY W. SCHULZE and F. ERDOGAN*
Lehigh University, Bethlehem, PA 18015, U.S.A.

(*Received* 27 *November* 1995; *in revised form* 3 *July* 1997)

Abstract—In this study the periodic cracking of an elastic coating bonded to a homogeneous substrate is considered. The problem is assumed to simulate the segmentation or "mud-flat" cracking of ceramic layers used as thermal barrier coatings in stationary and aircraft gas turbine engines. By expressing the displacements in terms of a combination of finite and infinite Fourier transforms, the corresponding mixed boundary value problem is reduced to an integral equation with the crack surface displacement as the unknown function. The main objective of the study is the examination of the influence of the length parameters c/b and b/h and the stiffness ratio μ_2/μ_1 on the crack tip stress intensity factors, the crack opening displacement, the strain energy released as a result of periodic cracking, and the in-plane tensile stress on the coating surface, where c, b, h, μ_1 and μ_2, respectively, are crack spacing, crack depth, coating thickness, shear modulus of the coating, and shear modulus of the substrate. The case of a periodically cracked strip is investigated separately and the stress intensity factors under fixed-load and fixed-grip conditions are compared. Also, the validity of the assumption made in simple energy balance calculations to the effect that the entire strain energy contained within the volume of the cell is released during periodic cracking is studied. It is shown that such an assumption is valid only for very small values of relative crack spacing c/b.

1. INTRODUCTION

Various ceramic coatings have been used in stationary and aircraft gas turbine engines for over twenty years to improve thermal efficiency and mechanical durability. In these applications the primary function of the coating has been the protection of metallic substrates against heat and corrosion (see, for example, Hodge *et al.*, 1980; Sumner and Ruckle, 1980; Grot and Martyn, 1981; Miller and Lowell, 1982; Pettit and Goward, 1983; Miller and Berndt, 1984; Sheffler and Gupta, 1988; Wortman *et al.*, 1989). Since the common coating materials such as partially stabilized ziconia are generally transparent to oxygen diffusion, very often a corrosion resistant bond coat (generally an NiCoCrAlY alloy) is also used as an interlayer between the coating and the substrate for shielding against corrosion. Field observations as well as laboratory tests indicate that the predominant mode of failure in these layered materials is spallation resulting from a crack in the ceramic coating parallel and close to the interface. The crack growth is driven by thermal excursions and, in some cases, very small amplitude and high frequency cyclic loading. Spallation is usually caused by the in-plane compression of the ceramic layer. However, the ceramic coating is also susceptible to surface cracking during the tensile part of the load cycle.

Surface cracks in ceramic components or coatings may be either a single dominant crack or a roughly regular array of periodic cracks (Grot and Martyn, 1981; Nied, 1990). This mud-flat type periodic cracking that occurs in ceramics is generally the consequence of residual stresses. Since the residual stresses are statically self-equilibrating, generally the cracks are relatively shallow surface cracks. From a practical viewpoint an important mechanics problem is finding a relationship between the magnitude of the external loads and the length parameter describing the crack periodicity for a given material characterized by its fracture toughness and other mechanical constants. A simple energy balance concept used for this purpose assumes that during the cracking process the total strain energy in the surface layer of depth b is released and is converted to fracture energy necessary for creating the cracks, where b is the crack depth (Nied, 1990). The configuration of cracks or the shape of the "cell" must be such that for a unit surface area the ratio of the released

* Author to whom correspondence should be addressed.

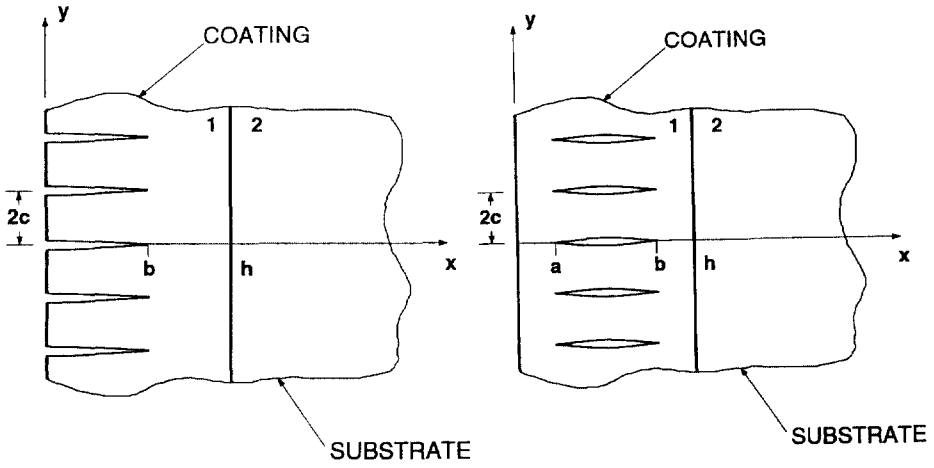

Fig. 1. Geometry of periodic cracks in elastic coatings.

energy to the dissipated energy is maximized (Nied, 1990; Erdogan and Ozturk, 1995). Thus, once the cell configuration is determined, the desired relationship between the cell size and the external load may be obtained from the energy balance given by

$$AbW = Sb\mathcal{G}_c/2 \tag{1}$$

where A is the surface area of the single cell, b is the crack depth, W is the strain energy density, S is the peripheral length of the crack in a single cell and $\mathcal{G}_c/2$ is the energy required to create a unit fracture surface. For example, if the medium is under biaxial tensile strain ε_0 near the surface, it may be shown that the cell is a regular hexagon having a side c, $A = 3\sqrt{3}(c^2/2)$, $S = 6c$, and from (1) we find

$$W = E\varepsilon_0^2/(1-\nu), \quad c\varepsilon_0^2 = \frac{2(1-\nu)}{\sqrt{3}E}\mathcal{G}_c. \tag{2}$$

Similarly, in plane problems described by Fig. 1a the cracking would take place perpendicular to maximum tensile stress and it may easily be shown that

$$W = \tfrac{1}{2}E\varepsilon_0^2, \quad c\varepsilon_0^2 = \mathcal{G}_c/E, \tag{3}$$

under plane stress conditions ($\sigma_{zz} = 0, \varepsilon_{yy} = \varepsilon_0$),

$$W = \tfrac{1}{2}E\varepsilon_0^2/(1-\nu^2), \quad c\varepsilon_0^2 = (1-\nu^2)\mathcal{G}_c/E \tag{4}$$

for plane strain case ($\varepsilon_{zz} = 0$, $\varepsilon_{yy} = \varepsilon_0$), and

$$W = \tfrac{1}{2}E(\varepsilon_1^2 + 2\nu\varepsilon_1\varepsilon_2 + \nu^2\varepsilon_2^2)/(1-\nu^2), c(\varepsilon_1^2 + 2\nu\varepsilon_1\varepsilon_2 + \nu^2\varepsilon_2^2) = (1-\nu^2)\mathcal{G}_c/E, \quad (\varepsilon_1 > \varepsilon_2) \tag{5}$$

for biaxial loading $\varepsilon_{yy} = \varepsilon_1$ and $\varepsilon_{zz} = \varepsilon_2$.

The method described above for estimating the cell size of periodic cracking from the magnitude of the external loads and the fracture toughness of the material is very useful for screening and for preliminary calculations. There are, however, a number of questions that need to be examined: How good is the assumption of total release of the strain energy in the cell? What is the actual stress intensity factor? How does the surface stress depend on the cell size? What is the influence of the crack depth? For arbitrary part geometries and loading conditions, the problem is highly complicated and these questions are very difficult

to study. However, if the part surface is relatively flat, then for general loading conditions for which the principal in-plane strains are biaxial and unequal, the local perturbation problem can be reduced to a plane strain problem shown in Fig. 1a and the periodic cracking problem can be analyzed.* For hexagonal cracking the problem is three-dimensional and analytically intractable.

In this study the somewhat more general problem of plane periodic cracking shown in Fig. 1b is considered. For $a = 0$ the problem reduces to the main surface crack problem given by Fig. 1a. Figure 1b can also be used to investigate the crack/contact problem in which near and at $x = 0$, because of residual compressive stresses, the crack surfaces may be in contact and the crack may form a cusp. The plane periodic crack problem for a homogeneous elastic half space was previously considered by Benthem and Koiter (1973), Bowie (1973), Nemat-Nasser *et al.* (1978) and Nied (1987). Two limiting cases of the problem shown in Fig. 1, namely a homogeneous layer and an elastic coating bonded to a rigid substrate, are obtained by substituting $\mu_2 = 0$ and $\mu_2 = \infty$, respectively, μ_2 being the shear modulus of the substrate.

2. THE FORMULATION

Consider the plane strain problem shown in Fig. 1b. We will assume that through a superposition the problem is reduced to a local perturbation problem in which self-equilibrating crack surface tractions are the only nonvanishing external loads. Because of periodicity, it is sufficient to consider the problem for $0 < y < c$ only. The equations of plane elasticity

$$(\kappa_i - 1)\nabla^2 u_i + 2\left(\frac{\partial^2 u_i}{\partial x^2} + \frac{\partial^2 v_i}{\partial x\,\partial y}\right) = 0,$$

$$(\kappa_i - 1)\nabla^2 v_i + 2\left(\frac{\partial^2 v_i}{\partial y^2} + \frac{\partial^2 u_i}{\partial x\,\partial y}\right) = 0, \quad (i = 1, 2) \tag{6}$$

would then have to be solved under the following boundary and continuity conditions:

$$\sigma_{1xy}(x, 0) = 0, \quad \sigma_{1xy}(x, c) = 0, \quad v_1(x, c) = 0, \quad 0 < x < h, \tag{7}$$

$$\sigma_{1xx}(0, y) = 0, \quad \sigma_{1xy}(0, y) = 0, \quad 0 < y < c, \tag{8}$$

$$\sigma_{2xy}(x, 0) = 0, \quad \sigma_{2xy}(x, c) = 0, \quad v_2(x, 0) = 0, \quad v_2(x, c) = 0, \quad h < x < \infty,$$
$$\sigma_{1xx}(h, y) = \sigma_{2xx}(h, y), \quad \sigma_{1xy}(h, y) = \sigma_{2xy}(h, y), \tag{9}$$

$$u_1(h, y) = u_2(h, y), \quad v_1(h, y) = v_2(h, y), \quad 0 < y < c, \tag{10}$$

$$\sigma_{1yy}(x, 0) = p(x), \quad a < x < b, \tag{11a}$$

$$v_1(x, 0) = 0, \quad 0 < x < a, \quad b < x < h \tag{11b}$$

where subscripts $i = 1$ and $i = 2$ refer to the coating and the substrate, respectively and $\kappa = 3\text{–}4\nu$ for plane strain and $\kappa = (3 - \nu)/(1 + \nu)$ for plane stress conditions. In (7)–(11) the symmetry conditions have been used and $p(x)$ is a known arbitrary function.

* In most applications the thickness of the substrate is much greater than that of the coating and the elastic constants of the bond coat are roughly the same as that of the substrate. Hence, the elasticity problem for the three-layer composite may closely be approximated by that of an elastic coating bonded to a semi-infinite elastic medium shown in Fig. 1.

By expressing the solution of (6) in terms of the sums of finite and infinite Fourier transforms, it can be shown that (Schulze, 1995)†

$$u_1(x,y) = \sum_{n=0}^{\infty} ((A_1 + A_2 x)\, e^{-\alpha_n x} + (A_3 + A_4 x)\, e^{\alpha_n x}) \cos(\alpha_n y)$$

$$+ \frac{1}{2\pi} \int_{-\infty}^{\infty} ((B_1 + B_2 y)\, e^{-|\beta| y} + (B_3 + B_4 y)\, e^{|\beta| y})\, e^{i x \beta}\, d\beta,$$

$$v_1(x,y) = \sum_{n=1}^{\infty} \left(\left(A_1 - \frac{\kappa_1}{\alpha_n} A_2 + A_2 x \right) e^{-\alpha_n x} - \left(A_3 + \frac{\kappa_1}{\alpha_n} A_4 + A_4 x \right) e^{\alpha_n x} \right) \sin(\alpha_n y)$$

$$+ \frac{1}{2\pi} \int_{-\infty}^{\infty} \frac{i}{\beta} ((|\beta| B_1 + \kappa_1 B_2 + |\beta| B_2 y)\, e^{-|\beta| y}$$

$$- (|\beta| B_3 - \kappa_1 B_4 + |\beta| B_4 y)\, e^{|\beta| y})\, e^{i x \beta}\, d\beta, \tag{12}$$

$$u_2(x,y) = \sum_{n=0}^{\infty} (C_{1n} + C_{2n} x)\, e^{-\alpha_n x} \cos(\alpha_n y),$$

$$v_2(x,y) = \sum_{n=1}^{\infty} \left(C_{1n} - \frac{\kappa_2}{\alpha_n} C_{2n} + C_{2n} x \right) e^{-\alpha_n x} \sin(\alpha_n y), \tag{13}$$

$$\alpha_n = \pi n / c. \tag{14}$$

From (13) and (14) it may be seen that conditions (9) are identically satisfied. The homogeneous conditions (7), (8) and (10) may be used to eliminate nine of the ten unknowns, the functions $A_i(\beta)$, $B_i(\beta)$, $(i = 1, \ldots, 4)$ and the set of constants C_{jn}, $(j = 1, 2)$, and the mixed boundary conditions (11) would then give the remaining one. If we define a new unknown function

$$f(x) = v_1(x, 0) \tag{15}$$

and let

$$f(x) = 0, \quad 0 < x < a, \quad b < x < h, \tag{16}$$

all ten unknowns can be expressed in terms of $f(x)$ and (11b) would be satisfied. Equation (11a) would then give an integral equation to determine $f(x)$.

Referring to Schulze (1995) for details, and to the Appendix, after some lengthy analysis the condition (11a) may be reduced to

$$\frac{1}{\pi} \int_a^b \left[\frac{1}{(s-x)^2} + k_{1s}(x,s) + k_{2s}(x,s) + k_f(x,s) \right] f(s)\, ds = \frac{\kappa_1 + 1}{4\mu_1} p(x), a < x < b, \tag{17}$$

where k_{1s} and k_{2s} are the standard generalized singular kernels given in the Appendix that become unbounded as x and s approach the free boundary $x = 0$ and the interface $x = h$, respectively, and the known function k_f contains unbounded terms that are, however, square-integrable in $0 \leqslant (x, s) \leqslant h$.

† From the expressions of the kernels given in the Appendix it may be seen that the terms involving $n = 0$ have no influence on the stresses [see (A3), (A6) and (A7)].

3. SOLUTION OF THE INTEGRAL EQUATION

By using the function-theoretic method (Muskhelishvili, 1953) and the properties of the strongly singular integral equations described by Kaya and Erdogan (1987a,b), it can be shown that the solution of (30) is of the following form:

$$f(s) = F(s)w_0(s), \quad w_0(s) = (s-a)^{\alpha}(b-s)^{\beta} \tag{18}$$

where $F(s)$ is a bounded function which is nonzero at $s = a$ and $s = b$ and the powers α and β in the weight function w_0 depend on the location of the crack tip. If the crack is fully embedded into the homogeneous medium 1 (Fig. 1b), that is, if $0 < a < b < h$, then $\alpha = \beta = 1/2$. If $a = 0$ (i.e., for the case of an edge crack), then $\alpha = 0$, and for $b = h$ (the crack terminating at the interface), β may be obtained from the following characteristic equation

$$-2\cos\pi\beta + m_1 + 12m_2\beta + 4m_2(\beta-1)(\beta-2) = 0, \quad 0 < \beta < 1, \tag{19}$$

where the bimaterial constants m_1 and m_2 are given by (A14) in the Appendix (Kaya and Erdogan, 1987b; Schulze 1995).

For numerical solution (17) is expressed in terms of the following normalized quantities:

$$s = \frac{b-a}{2}t + \frac{b+a}{2}, \quad x = \frac{b-a}{2}r + \frac{b+a}{2}, \quad -1 < (t, r) < 1,$$

$$f(s) = \frac{b-a}{2}\phi(t), \quad \frac{\pi(\kappa+1)}{4\mu_1}p(x) = g(r),$$

$$\left(\frac{b-a}{2}\right)^2 [k_{1s}(x,s), k_{2s}(x,s), k_f(x,s)] = [h_{1s}(r,t), h_{2s}(r,t), h_f(r,t)], \tag{20}$$

giving

$$\int_{-1}^{1} \left[\frac{1}{(t-r)^2} + h_{1s}(r,t) + h_{2s}(r,t) + h_f(r,t)\right]\phi(t)\,dt = g(r), \quad -1 < r < 1. \tag{21}$$

Also, from (18) and (20) it is seen that

$$\phi(t) = G(t)w(t), \quad w(t) = (1-t)^{\beta}(1+t)^{\alpha} \tag{22}$$

where $G(t)$ is the new unknown function. The orthogonal polynomials associated with the weight function $w(t)$ are the Jacobi polynomials and, in general (21) may be regularized and solved numerically by defining (Kaya and Erdogan, 1987a,b)

$$G(t) = \sum_{n=0}^{\infty} A_n P_n^{(\beta,\alpha)}(t). \tag{23}$$

In the special case of the embedded crack ($0 < a < b < h$), $\alpha = \beta = 1/2$ and (23) becomes

$$G(t) = \sum_{n=0}^{\infty} A_n U_n(t) \tag{24}$$

where U_n is the Chebyshev polynomial of the second kind. By observing that $(t-r)^{-2}$ is the only singular term in the kernel, the integral eqn (21) may thus be regularized by using the following relation (Kaya and Erdogan, 1987a):

$$\frac{1}{\pi}\int_{-1}^{1}\frac{U_n(t)\sqrt{1-t^2}}{(t-r)^2}\,dt = -(n+1)U_n(r), \quad n \geqslant 0, \quad |r| < 1. \tag{25}$$

For other combinations of α and β, the integral equation is solved by using the technique described by Kaya and Erdogan (1987a,b) and Mahajan (1991).

After evaluating the unknown function $f(x) = v_1(x,0)$, $a < x < b$, the mode I stress intensity factors may be defined by and calculated from

$$k_1(a) = \lim_{x\to a}\sqrt{2(a-x)}\sigma_{1yy}(x,0) = \frac{4\mu_1}{\kappa_1+1}\lim_{x\to a}\frac{v_1(x,0)}{\sqrt{2(x-a)}}$$

$$= \frac{4\mu_1}{\kappa_1+1}F(a)\sqrt{\frac{b-a}{2}},$$

$$k_1(b) = \lim_{x\to b}\sqrt{2(x-b)}\sigma_{1yy}(x,0) = \frac{4\mu_1}{\kappa_1+1}\lim_{x\to b}\frac{v_1(x,0)}{\sqrt{2(b-x)}}$$

$$= \frac{4\mu_1}{\kappa_1+1}F(b)\sqrt{\frac{b-a}{2}}. \tag{26}$$

Equations (26) are valid for $0 < a < b < h$. For an edge crack $a = 0$ we have $\alpha = 0$, $w_0 = \sqrt{b-x}$, $v_1(x,0) = f(x) = F(x)\sqrt{b-x}$ and from (26b) it may be seen that

$$k_1(b) = \frac{4\mu_1}{\kappa_1+1}\frac{F(b)}{\sqrt{2}}. \tag{27}$$

Similarly, for a crack terminating at the interface, around the crack tip $x = b = h$ we have $v_1(x,0) \sim (h-x)^{\beta}$ and $\sigma_{2yy}(x,0) \sim (1/(x-h)^{1-\beta})$ and referring to (18) the strength of the stress singularity may again be evaluated in terms of the constant $F(h)$ (see Kaya and Erdogan, 1987b for details).

Once the crack surface displacement $v_1(x,0)$ is determined, the released strain energy per unit cell $(-c < y < c, -\frac{1}{2} < z < \frac{1}{2})$ may be obtained from

$$V = -2\int_0^b \frac{1}{2}\sigma_{1yy}(x,0)v_1(x,0)\,dx = -\int_0^b p(x)f(x)\,dx. \tag{28}$$

If we now observe that the number of cells per unit length in y direction is $1/2c$, the released strain energy per unit surface area of coating becomes

$$V_1 = \frac{V}{2c} = -\frac{1}{2c}\int_0^b p(x)f(x)\,dx. \tag{29}$$

This should be compared with the strain energy U_1 contained within the volume $(0 < x < b, -\frac{1}{2} < y < \frac{1}{2}, -\frac{1}{2} < z < \frac{1}{2})$ of the uncracked coating given by

$$U_1 = bW \tag{30}$$

where, for each relevant loading condition W is obtained from (3)–(5).

Finally, a quantity of considerable practical interest is the surface stress $\sigma_{1yy}(0,y)$, $0 < y \leqslant c$, as it may have a bearing on further cracking or cell division. Referring to (A1) the stress on the coating surface perpendicular to the plane of the crack may be expressed as

$$\sigma_{1yy}(0,y) = \frac{\mu_1}{\kappa_1+1}\int_a^b [K_1(0,y,s)+K_2(0,y,s)]f(s)\,ds, \quad 0 < y \leqslant c \tag{31}$$

where the kernels K_1 and K_2 are given by (A2) and (A3), respectively. It should be noted that (31) would give the stress for the perturbation problem solved under the conditions (7)–(11). To obtain the correct stress, σ_{1yy} given by the solution of the uncracked medium under prescribed external loads must be added to that given by (31).

4. RESULTS

In the formulation given in this study the substrate or medium 2 is semi-infinite. Therefore, the composite medium is fully constrained against rotation and in the uncracked medium we always have $\varepsilon_{1yy} = \varepsilon_{2yy} = \varepsilon_0$. If the medium is loaded mechanically, the crack surface tractions to be used in the solution of the perturbation problem would be

$$\sigma_{1yy}(x,0) = p(x) = -p_0, \quad \sigma_{1xy}(x,0) = 0 \tag{32}$$

where

$$p_0 = E_1\varepsilon_0 \tag{33}$$

for plane stress loading $\sigma_{1zz} = 0, \varepsilon_{1yy}(x, \mp\infty) = \varepsilon_0$, and

$$p_0 = \frac{E_1\varepsilon_0}{1-\nu_1^2} \tag{34}$$

for plane strain loading $\varepsilon_{1zz} = 0$, $\varepsilon_{1yy}(x, \mp\infty) = \varepsilon_0$, and

$$p_0 = \frac{E_1}{1-\nu_1^2}(\varepsilon_1+\nu_1\varepsilon_2) \tag{35}$$

for biaxial loading $\varepsilon_{1yy}(x, \mp\infty) = \varepsilon_1$, $\varepsilon_{1zz}(x,y) = \varepsilon_2$, $\varepsilon_1 > \varepsilon_2$. All results given in this section are obtained for a constant value of and are normalized with respect to p_0. For more complex loading conditions such as thermal shock, $p(x)$ would be a given function obtained from the solution of the uncracked medium. Also, the numerical results presented in this study are obtained by assuming that $\nu_1 = \nu_2 = 0.3$.

Some sample results giving the normalized crack surface displacement $\delta(x) = v_1(x,0)/V_0$ for an edge crack are shown in Figs 2 and 3. The normalizing factor

$$V_0 = \frac{1+\kappa_1}{4\mu_1}p_0 b \tag{36}$$

is the surface displacement at the center of a crack of length $2b$ in an infinite plane under uniform tension p_0 perpendicular to the plane of the crack. Figure 2 shows the effect of $b/2c$ on the crack surface displacement for $h = \infty$. For fixed values of $b/2c = 0.5$ and $b/h = 0.9$, the effect of the stiffness ratio μ_2/μ_1 is shown in Fig. 3. The main result of these figures and other examples considered by Schulze (1995) is that the dominant factor on the crack surface displacement $v_1(x,0)$ is the b/c ratio, $v_1(x,0) \to 0$ as $c \to 0$, and the influence of the crack depth b/h and the stiffness ratio μ_2/μ_1 is relatively small.

Figures 4–12 show the calculated mode I stress intensity factors $k_1(b)$ for the important case of surface cracks. Some embedded crack results are given by Schulze (1995). The results are normalized with respect to $p_0\sqrt{l}$, where p_0 is given by (33)–(35) and $l = b$ is the crack length. Figure 4 shows the effect of crack spacing c $(0 < c < \infty)$ on the stress intensity factor in a homogeneous half plane. This is a known result reproduced here for verification

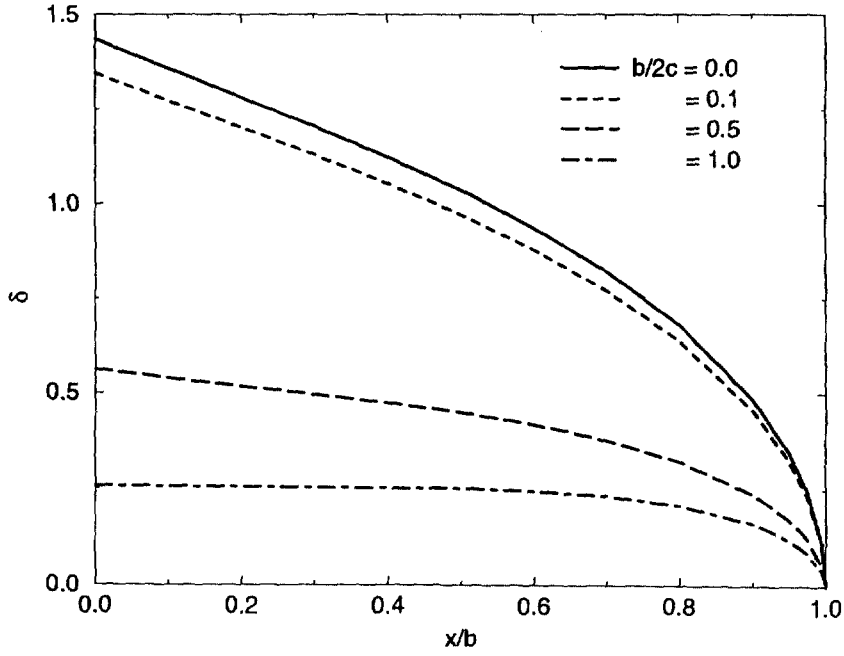

Fig. 2. Normalized crack surface displacement in a half plane with periodic edge cracks, $\delta = v_1(x, 0)/V_0$, $V_0 = p_0 b(1+\kappa_1)/4\mu_1$.

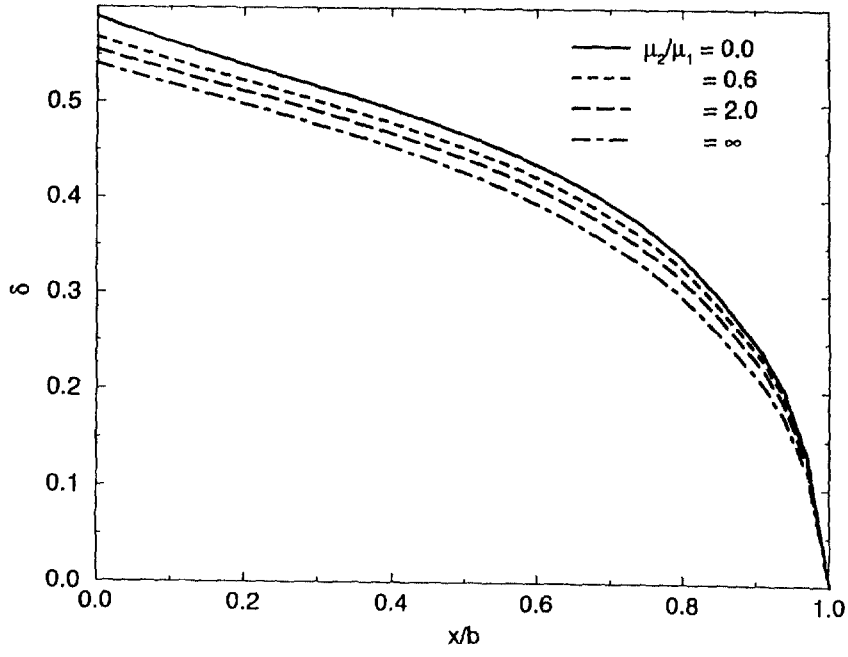

Fig. 3. Normalized crack surface displacement in elastic coatings, $b/2c = 0.5$, $b/h = 0.9$, $\delta = v_1(x, 0)/V_0$, μ_1, μ_2: shear moduli (see Fig. 1a).

(Nied, 1987). Note that $k_1(b) \to 0$ for $c \to 0$ and $k_1(b) \to 1.1215\, p_0\sqrt{l}$ for $c \to \infty$, the latter being the well-known single edge crack result. For a single edge crack ($c = \infty$), the effect of the stiffness ratio μ_2/μ_1 and the relative crack depth b/h is shown in Fig. 5. It may be seen that as $b \to h$, $k_1(b)$ becomes unbounded for $\mu_2 < \mu_1$ and tends to zero for $\mu_2 > \mu_1$, which are the known expected trends. For various stiffness ratios μ_2/μ_1, the effect of relative crack spacing b/c and relative crack length b/h is shown in Figs 6–9. Figures show that, except

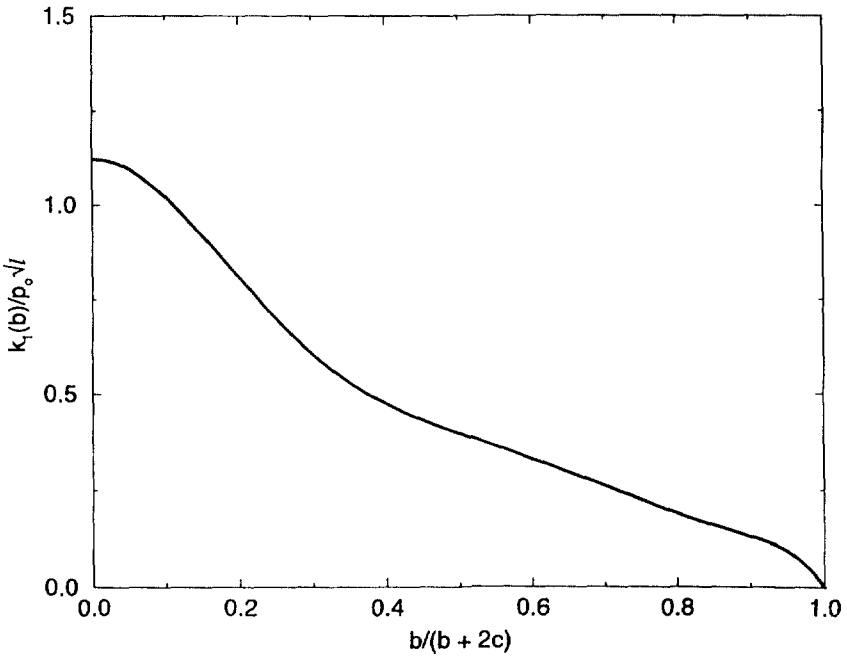

Fig. 4. Normalized stress intensity factor in an elastic half plane with periodic surface cracks, $l = b$.

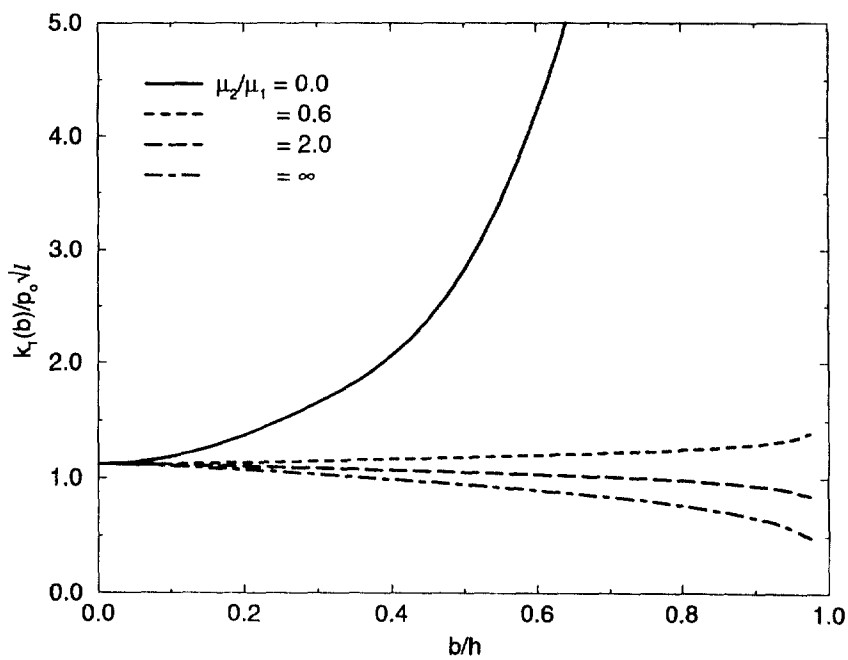

Fig. 5. Influence of the stiffness ratio μ_2/μ_1 on the stress intensity factor in an elastic coating with a single edge crack, $c = \infty$, $l = b$.

around $b = h$, the dependence of k_1 on b is nearly parabolic, as in the case of uniformly loaded infinite plane ($k_1 = p_0\sqrt{b}$). This may be seen somewhat better in Fig. 10 where $k_1(b)$ is normalized with respect to a constant $p_0\sqrt{h}$. For fixed values of crack spacing $b/2c = 0.5$ and $b/2c = 0.1$, Figs 11 and 12 show the effect of stiffness ratio and relative crack depth on the stress intensity factor. From these results one may conclude that the dominant factor in the variation of the stress intensity factors appears to be the relative crack spacing.

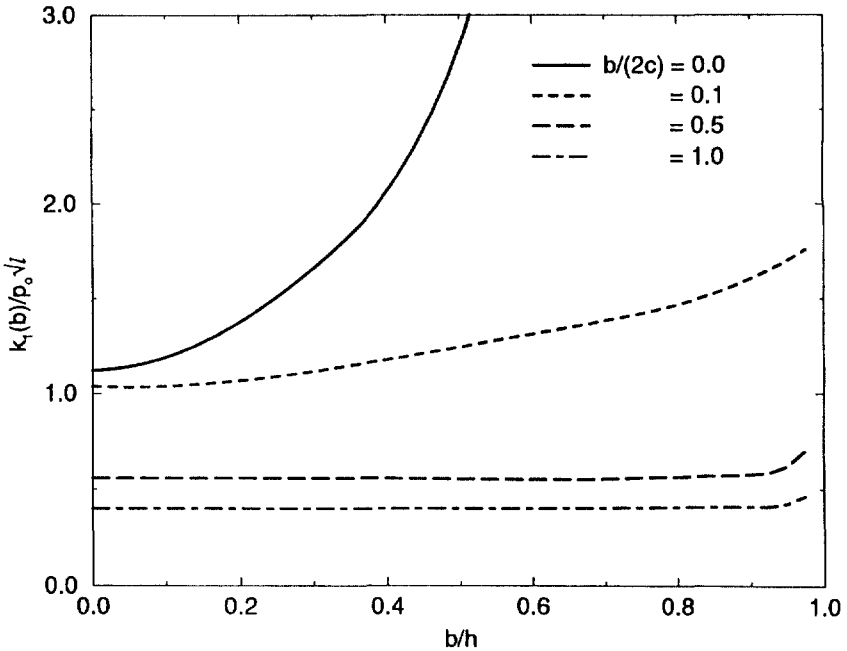

Fig. 6. Normalized stress intensity factor in an elastic strip under constant strain loading with periodic cracks, $\mu_2 = 0$, $l = b$.

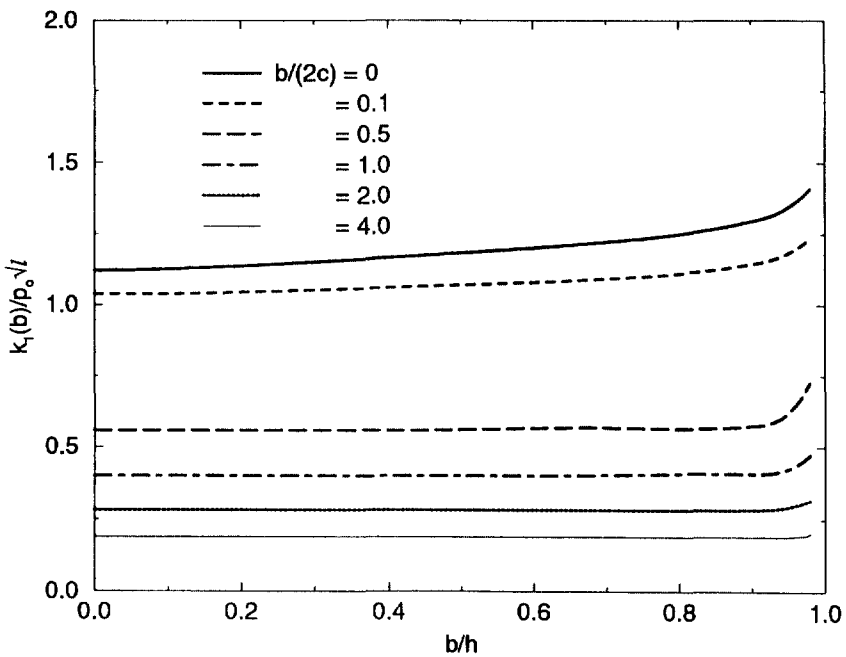

Fig. 7. Normalized stress intensity factor in a periodically cracked elastic coating, $\mu_2/\mu_1 = 0.6$, $l = b$.

In the formulation of periodic surface crack problems, for $\mu_2 \neq 0$ the external load is generally a constant strain applied at infinity through "fixed grips". However, in the case of a strip with periodic cracks (i.e., for $\mu_2 = 0$), the loading may be either constant strain $\varepsilon_{1yy} = \varepsilon_0$ or constant resultant force $p_0 h$ applied at $y = \mp\infty$. The results given in this study for $\mu_2 = 0$ as well as $\mu_2 > 0$ are for constant strain loading. To explain the difference, consider a strip $0 < x < h$, load it in the y direction so that $\varepsilon_{yy} = \varepsilon_0$, fix the grip at $y = \mp\infty$ while under load, then introduce a series of periodic cuts along $0 < x < b$, $y = \mp 2cn$,

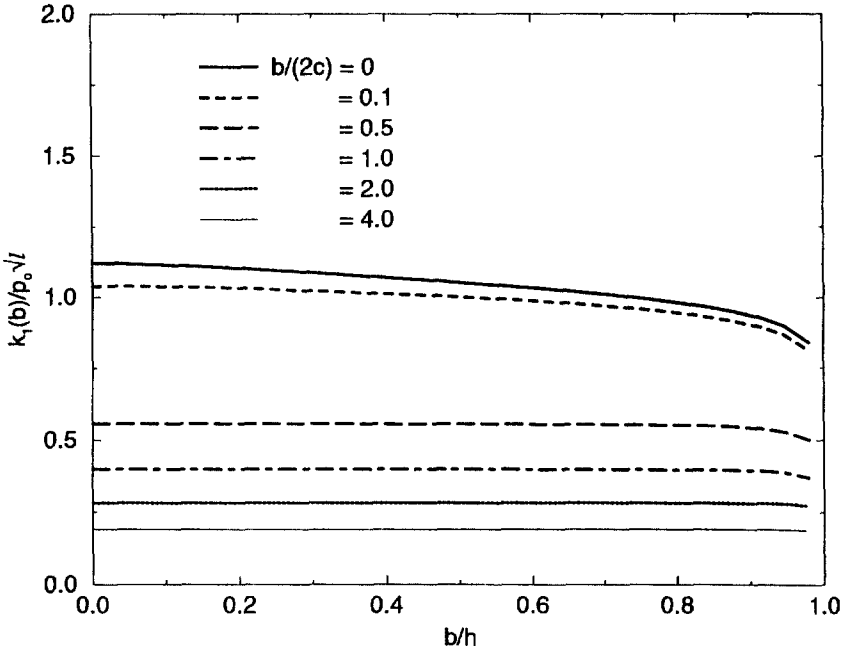

Fig. 8. Normalized stress intensity factor in a periodically cracked elastic coating, $\mu_2/\mu_1 = 2$, $l = b$.

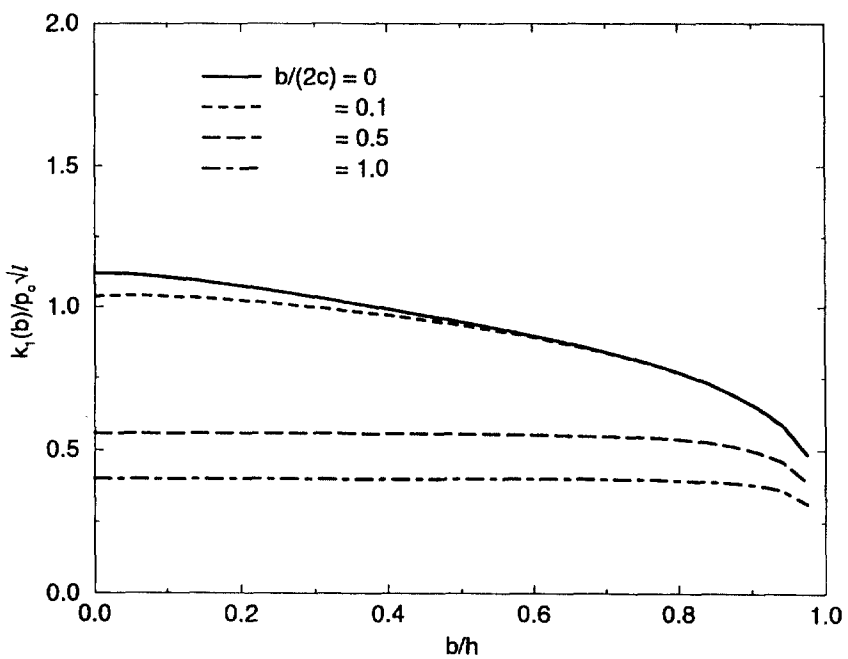

Fig. 9. Normalized stress intensity factor in a periodically cracked elastic coating, $\mu_2/\mu_1 = \infty$, $l = b$.

$n = 0, 1, 2, \ldots$ This would cause a reduction in the magnitude of the resultant force (or in the average stress) in the y direction, while the average strain would remain constant at ε_0. On the other hand, during the process of introducing the cracks if we do not constrain the ends and keep the resultant force constant (e.g., through a dead weight), there would be an increase in the average strain in the y direction, while the average stress would remain unchanged. Clearly, the stress intensity factor for the fixed load case would be greater than the fixed strain case. Since the basic geometry and nature of the boundary conditions are

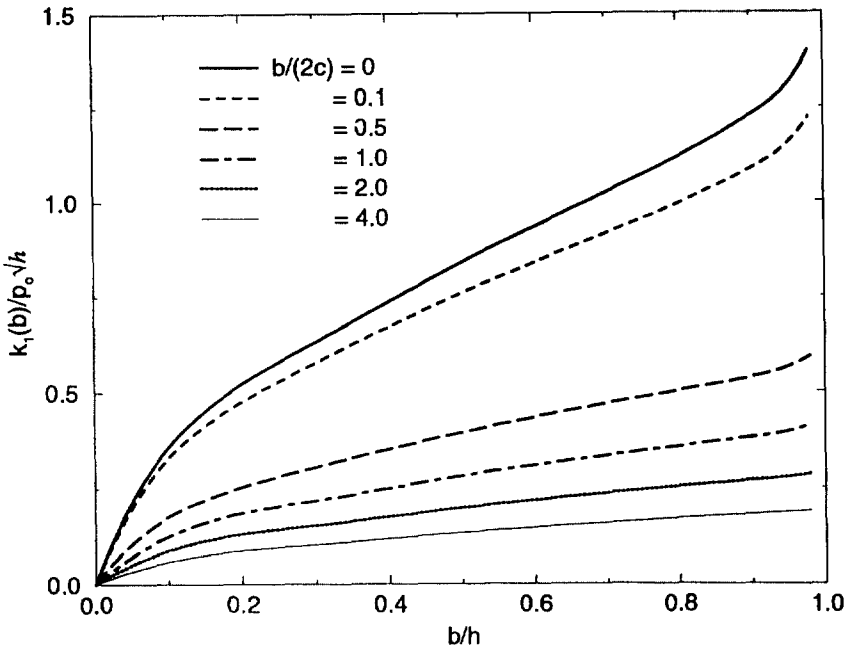

Fig. 10. Stress intensity factor in a periodically cracked elastic coating normalized with respect to a constant $p_0\sqrt{h}$. $\mu_2/\mu_1 = 0.6$.

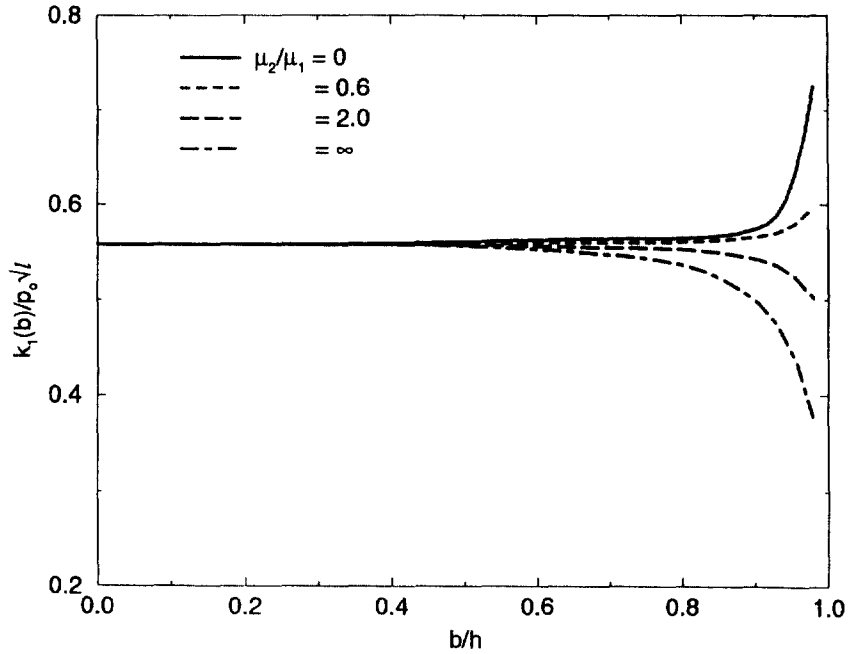

Fig. 11. The effect of the stiffness ratio μ_2/μ_1 on the normalized stress intensity factor in periodically cracked elastic coatings. $b/2c = 0.5$.

the same for both cases, from the perturbation solution given in this study for the constant strain case it should be possible to obtain the results for the fixed load problem. To show this, we consider the superposition described in Fig. 13 for a half cell. In all three problems shown $\sigma_{xy}(x, 0) = 0$, $\sigma_{xy}(x, c) = 0$ and $\sigma_{yy}(x, c)$ is such that $v(x, c)$ is independent of x. Along the shaded boundaries $v(x, 0) = 0$. From superposition it then follows that

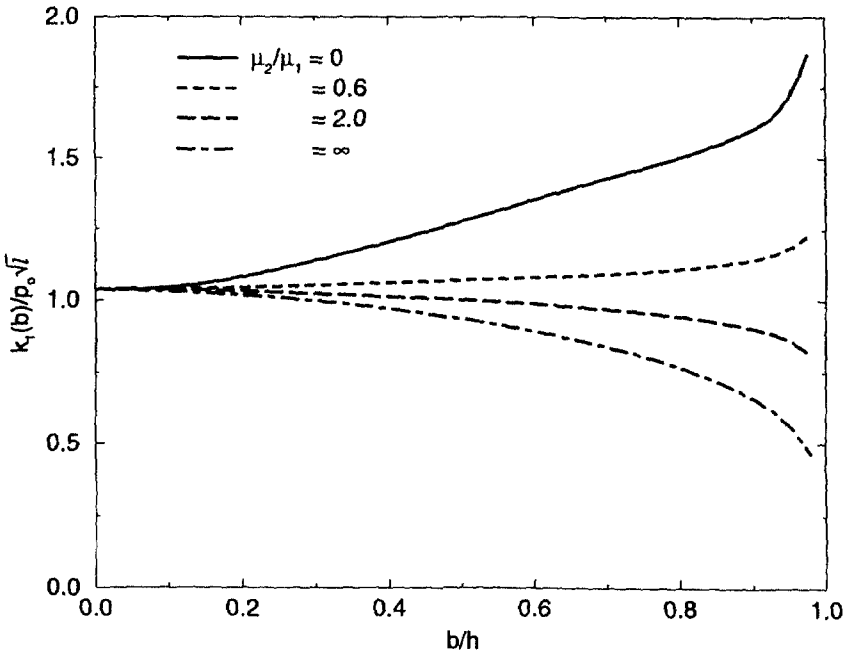

Fig. 12. The effect of the stiffness ratio μ_2/μ_1 on the normalized stress intensity factor in periodically cracked elastic coatings, $b/2c = 0.1$.

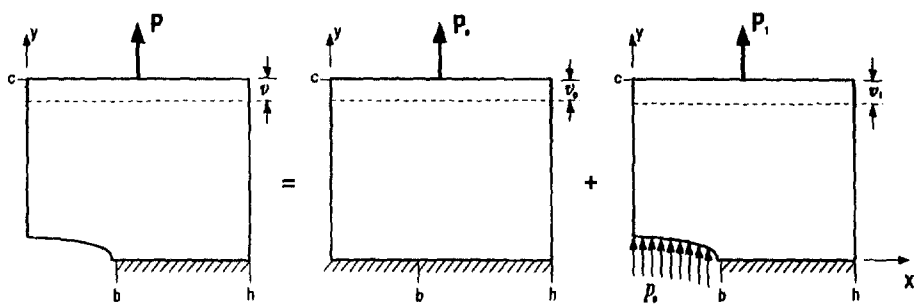

Fig. 13. General description of superposition in an elastic strip with periodic edge cracks.

$$P = P_0 + P_1, \quad v = v_0 + v_1. \tag{37}$$

Referring to Fig. 13, for the fixed grip case we have

$$v = v_0, \quad v_1 = 0, \quad \varepsilon_0 = v_0/c, \quad P_0 = hp_0, \quad P = P_\varepsilon = P_0 + P_1,$$
$$P_1 = -p_0 b + \int_0^h \sigma_{yy}(x, 0)\,dx = \int_0^h \sigma_{yy}(x, c)\,dx. \tag{38}$$

The third figure with $v_1 = 0$ corresponds to the perturbation problem considered in this study. Note that since $v_1 = 0$ and the applied load p_0 is compressive, the resultant force P_1 is expected to be negative. In this case the known quantity is ε_0 and p_0 is given by (33) or (34).

In the case of fixed load the known quantity is p_0 or $P = P_\sigma = hp_0$ and

$$P = P_\sigma = P_0 + P_1, \quad v = v_0 + v_1, \quad P_0 = hp_0, \quad P_1 = 0, \quad v_0 = c\varepsilon_0, \tag{39}$$

where ε_0 is related to p_0 through (33) or (34) and v_1 is an unknown positive constant.

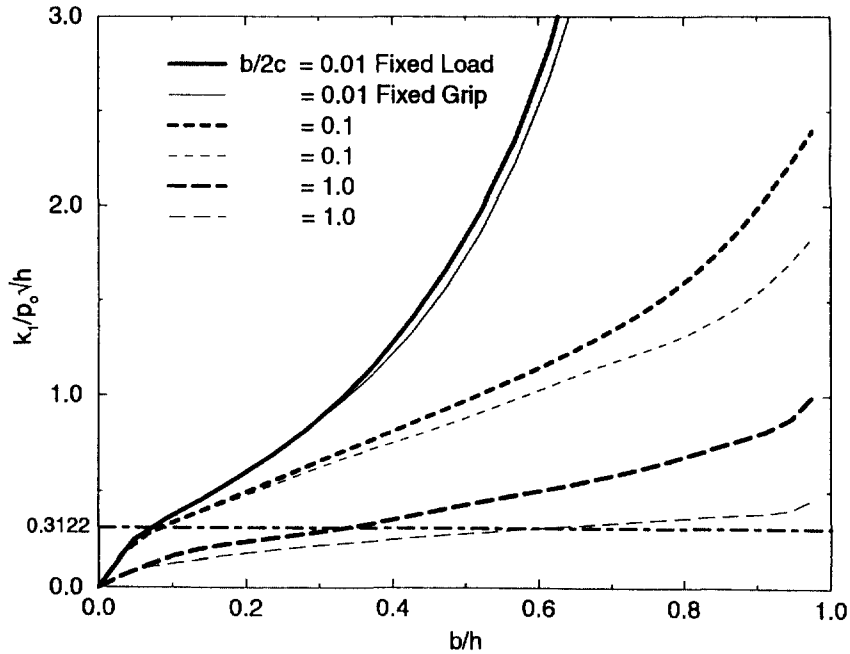

Fig. 14. Comparison of stress intensity factors for a periodically cracked elastic strip under fixed strain and fixed load conditions.

In the problem under consideration the uncracked solution corresponding to the middle configuration in Fig. 13 is the same for both fixed grip and fixed load cases. The configuration on the left describes the real problem where in the fixed grip case $v = v_0$, $P = P_\varepsilon < P_0$ and in the fixed load case $P = P_\sigma = P_0$, $v > v_0$. In both cases since P is the magnitude of the applied loads, the stress intensity factor may be expressed as

$$k_1(b) = Pf_0\left(\frac{b}{h}, \frac{c}{h}\right) \tag{40}$$

where the function f_0 depends only on the geometry and the material constants. If the stress intensity factor $k_{1\varepsilon}$ for the fixed grip case is known, then from (40) and (38) the stress intensity factor $k_{1\sigma}$ for the fixed load case may be obtained as follows:

$$k_{1\sigma}(b) = \frac{P_\sigma}{P_\varepsilon} k_{1\varepsilon}(b), \tag{41}$$

$$\frac{P_\sigma}{P_\varepsilon} = \frac{p_0 h}{p_0 h - p_0 b + \int_b^h \sigma_{yy}(x, 0)\,\mathrm{d}x} = \frac{p_0 h}{p_0 h + \int_0^h \sigma_{yy}(x, c)\,\mathrm{d}x}, \tag{42}$$

where $\sigma_{yy}(x, y)$ used in (42) is evaluated from the fixed-grip perturbation problem (third configuration in Fig. 13 with $v_1 = 0$) and, again p_0 and ε_0 are related through (33) or (34).

Considerations similar to (41) apply to all other calculated quantities given in this study. For example, the stress intensity factors $k_1(a)$ and $k_1(b)$ for the embedded cracks, the crack surface displacement $v_1(x, 0) = f(x)$ and the surface stress $\sigma_{yy}(0, y)$ under fixed load conditions may be calculated by multiplying the quantities obtained from, respectively, (26), (17) and (31) under constant strain loading by P_σ/P_ε ratio [given by (42)]. Also note that the ratio P_ε/P_σ gives the reduction in the stiffness in the y direction due to periodic cracking, that is $P_\varepsilon/P_\sigma = E_{\mathrm{av}}/E$ where E_{av} is the average longitudinal stiffness of the cracked strip.

Figure 14 shows the comparison of the stress intensity factors in a periodically cracked elastic strip under fixed grip and fixed load conditions. Note that the difference becomes

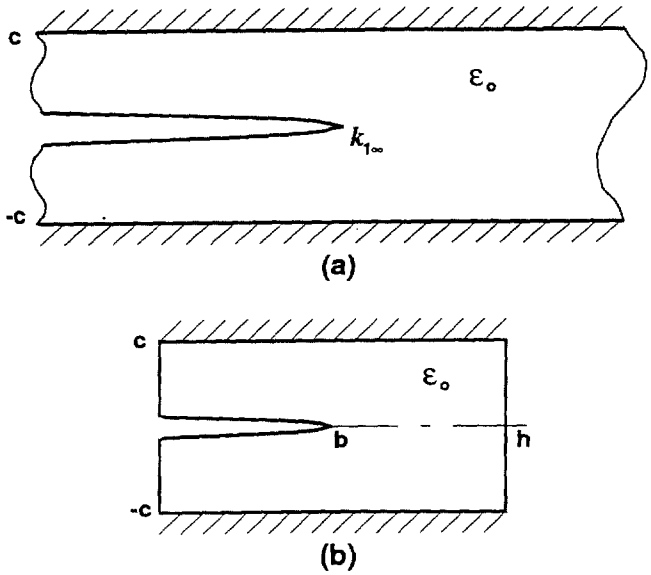

Fig. 15. Geometry of a single cell in a periodically cracked infinite plane ($h = \infty, b = \infty$) and a strip with finite thickness h, $b = h/2$.

quite significant as the relative crack spacing $2c/b$ decreases. Another interesting comparison of the fixed-grip stress intensity factor for very small values of c may be made with the exact solution obtained from tearing of a long strip or an infinite medium containing semi-infinite periodic cracks under constant strain loading (Fig. 15). In the infinite strip shown in Fig. 15a, using energy balance considerations, the stress intensity factor may be calculated as

$$k_{1\infty} = 2\mu\varepsilon_0\sqrt{\frac{2c}{\pi(\kappa-1)}} = p_0(1-\nu)\sqrt{\frac{c}{\pi(1-2\nu)}}, \tag{43}$$

from which, for $\nu = 0.3$, it follows that

$$\frac{k_{1\infty}}{p_0\sqrt{c}} = 0.6244, \quad \text{or} \quad \frac{k_{1\infty}}{p_0\sqrt{h}} = 0.6244\sqrt{\frac{c}{h}}. \tag{44}$$

In the periodic crack examples shown in Fig. 14, the configuration closest to Fig. 15a (or that with smallest c) is $b/2c = 1$, which at $b/h = 0.5$, gives $c/h = 1/4$ or $k_{1\infty}/p_0\sqrt{h} = 0.3122$. Figure 14 shows that around $b/h = 0.5$ this result agrees rather well with the periodic crack solution.

Some sample results showing the released strain energy as a result of periodic surface cracking of elastic coatings under fixed strain loading are given in Figs 16 and 17. Figure 16 shows the normalized strain energy V_1/U_1 for $b/h = 0.9$ and various values of μ_2/μ_1 as a function of the crack spacing c/b, where V_1 and U_1 have been evaluated from (29) and (30), respectively. Similarly, the influence of b/h, μ_2/μ_1 and c/b on V_1/U_1 is shown in Fig. 17. The simple energy balance concept used in estimating the crack spacing for a given loading ε_0 [see (3)–(5)] is based on the assumption that $V_1 = U_1$. The figures indicate that the assumption is valid only for very small values of c and becomes progressively worse as μ_2/μ_1 and c/b increase and as b/h decreases.

Finally, Figs 18–20 show the distribution of the surface stress $\sigma_{1yy}(0, y)$ in the coating, again under fixed-grip loading conditions. Figure 18 shows the result for a homogeneous half plane. The surface stress for a coating bonded to a rigid substrate is shown in Fig. 19 and the effect of the stiffness ratio μ_2/μ_1 is described in Fig. 20. Note that at $y = 0$ the stress

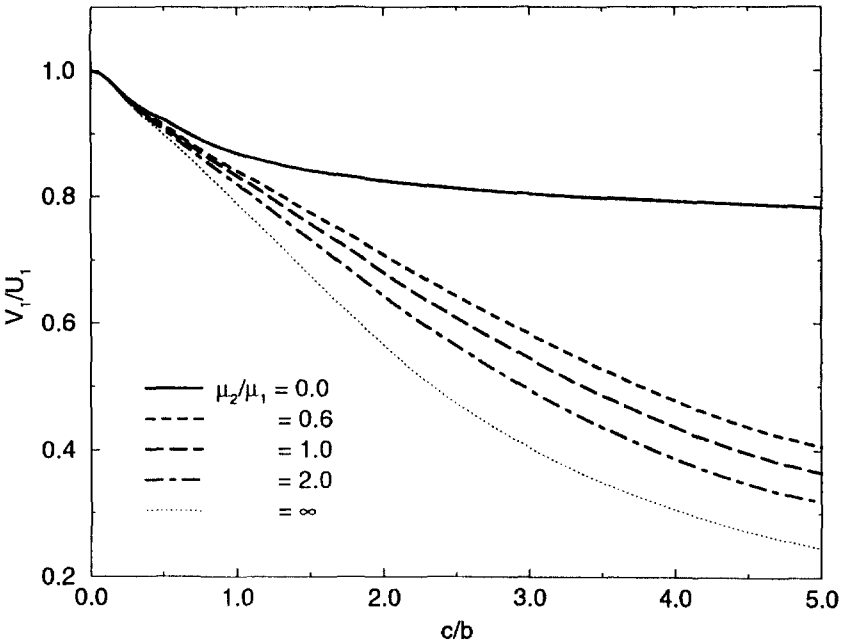

Fig. 16. Influence of the stiffness ratio μ_2/μ_1 on the normalized strain energy released as a result of periodic cracking, $b/h = 0.9$.

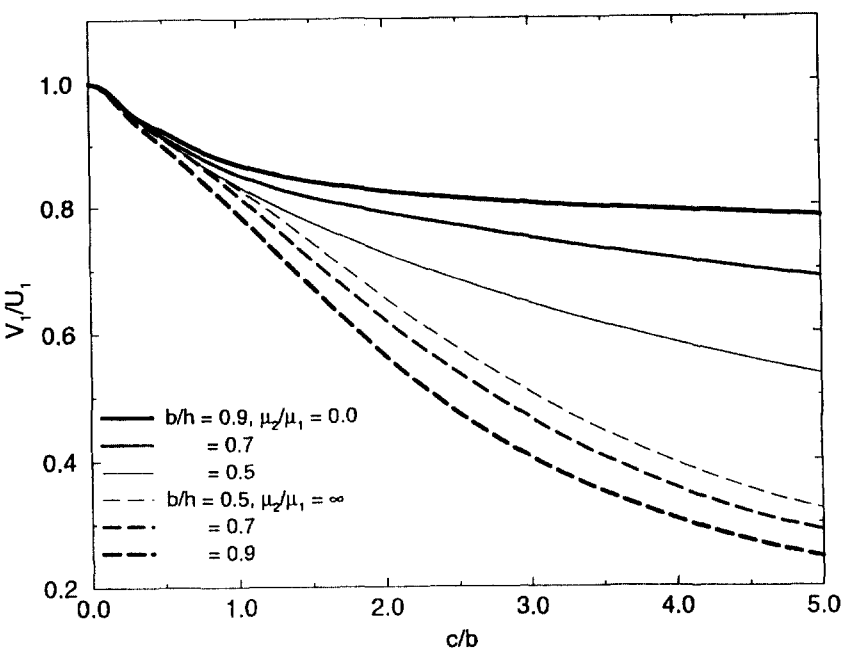

Fig. 17. Influence of μ_2/μ_1 and b/h on the normalized strain energy released during periodic cracking.

is zero and, as expected, monotonically increases with increasing y. Also the surface stress tends to increase with increasing crack spacing c/b, decreasing crack length and increasing substrate stiffness μ_2/μ_1.

5. CONCLUDING REMARKS

Observing that the problem is linear, the results found in this study may be applied to any combination of mechanical, thermal and residual biaxial stresses by using superposition.

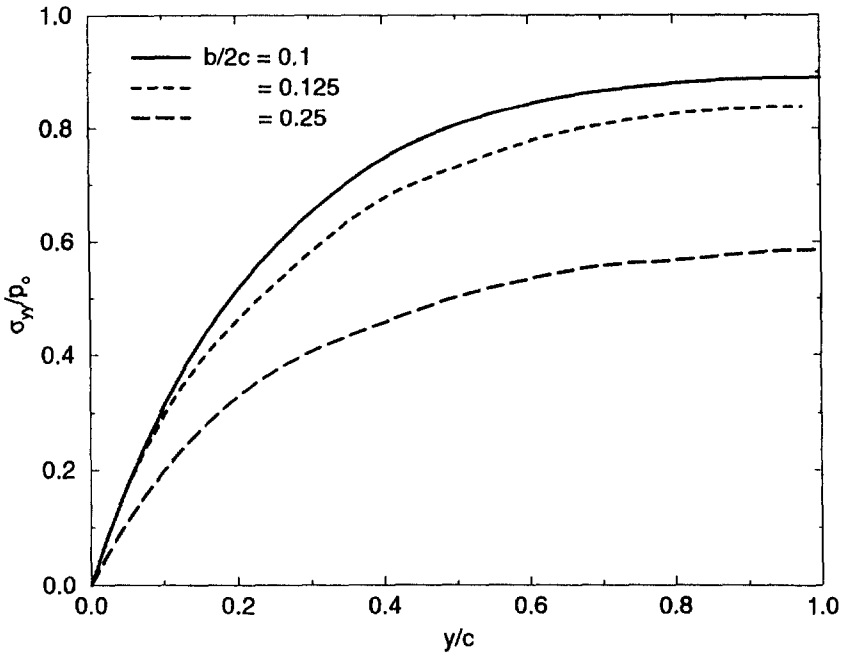

Fig. 18. The distribution of the surface strain $\sigma_{yy}(0, y)$ in a periodically cracked half plane.

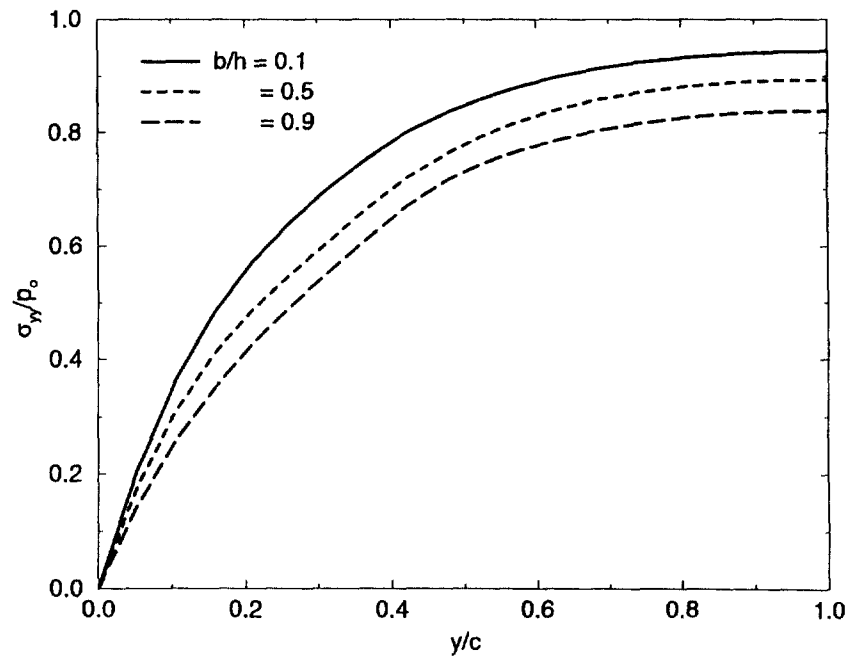

Fig. 19. The distribution of surface stress $\sigma_{1yy}(0, y) = \sigma_{yy}$ in a periodically cracked elastic coating bonded to a rigid substrate, $\mu_2 = \infty$, $b/2c = 0.125$.

In formulating the problem the crack surface tractions have been used as the external load. To obtain the actual stress state in the medium the solution of the problem in the absence of periodic cracks needs to be superimposed on the stresses found in this study. However, this would not have any influence on the stress intensity factors and the crack surface displacements. It should also be pointed out that the crack surface tractions used in the formulation are arbitrary functions of the depth coordinate x. Therefore, the technique

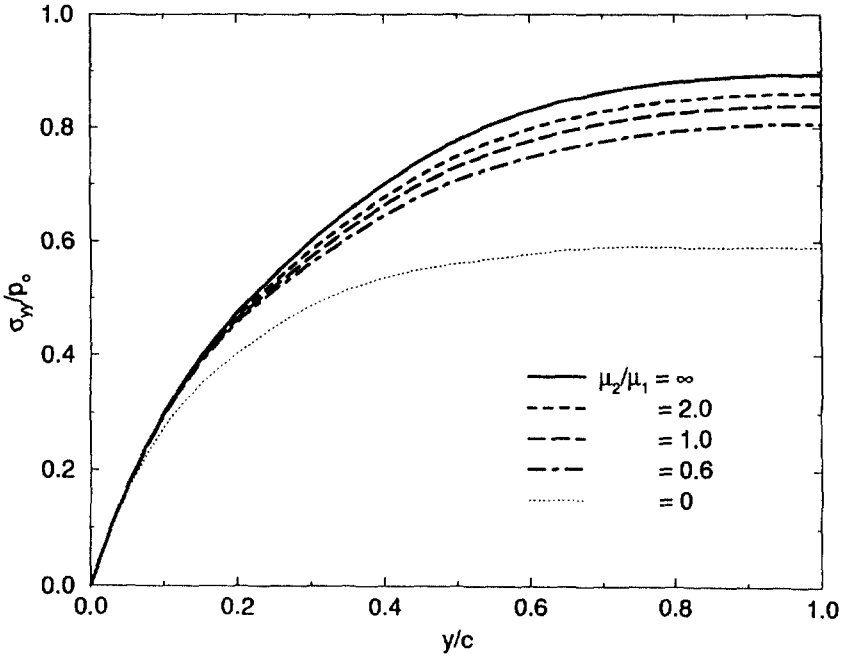

Fig. 20. The influence of the stiffness ratio μ_2/μ_1 on the surface stress $\sigma_{1yy}(0, y) = \sigma_{1y}$ in a periodically cracked elastic coating, $b/h = 0.5$, $b/2c = 0.125$.

developed is readily applicable to surface cracking caused by external loads that would give in-plane stresses in the coating which are not uniform. An important practical problem that can be studied by using this technique would be the periodic surface cracking of the coating under thermal shock conditions. In solving this and other transient problems one would, of course, have to assume that the inertia effects are negligible.

In closing it may be observed that the method developed and the results found in this study may be applicable to periodic cracking of any fully constrained and biaxially loaded coating/substrate system in which $h_1 \ll h_2$ and the in-plane principal strains are unequal, where h_1 and h_2 are the thicknesses of the coating and the substrate, respectively. This includes nearly all composite plate and shell problems under quasi-static mechanical and thermal loading.

Acknowledgements—This study was supported by the ONR under the Grant N00014-93-1-0557 and by AFOSR under the Grant F49620-93-1-0252. The authors are also grateful to the General Motors Corporation for the GM Graduate Fellowship.

REFERENCES

Benthem, J. P. and Koiter, W. T. (1973) Asymptotic approximations to crack problems. In *Mechanics of Fracture, Methods of Analysis and Solutions of Crack Problems*, ed. G. C. Sih, pp. 131–178. Noordhoff, Leyden, The Netherlands.

Bowie, O. L. (1973) Solutions of plane crack problems by mapping technique. In *Mechanics of Fracture, Methods of Analysis and Solutions of Crack Problems*, ed. G. C. Sih, pp. 1–55. Noordhoff, Leyden, The Netherlands.

Erdogan, F. and Ozturk, M. (1995) Periodic cracking of functionally graded coatings. *Int. J. Engng. Sci.* **33**, 2179–2195.

Grot, A. S. and Martyn, J. K. (1981) Behavior plasma-sprayed ceramic thermal barrier coating for gas turbine engines. *The Bulletin of the American Cer. Soc.* **60**(8), 807–811.

Hodge, P. E., Miller, R. A. and Gedwill, M. A. (1980) Evaluation of hot corrosion behavior of thermal barrier coatings. *Thin Solid Films* **73**(2), 447–453.

Kaya, A. C. and Erdogan, F. (1987a) On the solution of integral equations with strongly singular kernels. *Quarterly of Applied Mathematics* **XLV**, 105–122.

Kaya, A. C. and Erdogan, F. (1987b) On the solution of integral equations with a generalized Cauchy kernel. *Quarterly of Applied Mathematics* **XLV**, 455–469.

Mahajan, R. V. (1991) Contact and crack problems for an orthotropic half plane stiffened by elastic films. Ph.D. dissertation, ME/MECH Department, Lehigh University.

Miller, R. A. and Berndt, C. C. (1984) Performance of thermal barrier coatings in high heat flux environments. *Thin Solid Films* **119,** 195–202.
Miller, R. A. and Lowell, C. E. (1982) Failure of thermal barrier coatings exposed to elevated temperature. *Thin Solid Films* **95,** 265–273.
Muskhelishvili, N. I. (1953) *Singular Integral Equations*. Noordhoff, Groningen, The Netherlands.
Nemat-Nasser, S., Keer, L. M. and Parihar, K. S. (1978) Unstable crack growth of thermally induced interacting cracks in brittle solids. *International Journal of Solids and Structures* **14,** 409–430.
Nied, H. A. (1990) Criterion for predicting segmentation cracking on surfaces of brittle materials. GE/CRD Report 90CRD258.
Nied, H. F. (1987) Periodic array of cracks in a half plane subjected to arbitrary loading. *ASME Journal of Applied Mechanics* **54,** 642–648.
Pettit, F. S. and Goward, G. W. (1983) High temperature corrosion and use of coatings for protection. *Metallurgical Treatises, Metallurgical Society of AIME*, pp. 603–619.
Schulze, G. W. (1995) Periodic cracking of elastic coatings. Ph.D. dissertation, ME/MECH Department, Lehigh University.
Sheffler, K. D. and Gupta, D. K. (1988) Current status and future trends in turbine application of thermal barrier coatings. *ASME Journal of Engineering, Gas Turbine Power* **110,** 605–609.
Sumner, I. E. and Ruckle, D. L. (1980) Development of improved durability plasma sprayed ceramic coatings for gas turbine engines. AIAA paper No. 80-1193.
Wortman, D. J., Nagaraj, D. A. and Duderstadt, E. C. (1989) Thermal barrier coatings for gas turbine use. *Materials Science and Engineering, A* **121,** 433–440.

APPENDIX

Referring to Schulze (1995), the mixed boundary condition (11a) may be expressed as

$$\frac{\kappa_1+1}{\mu_1}p(x)=\lim_{y\to 0}\int_a^b [K_1(x,y,s)+K_2(x,y,s)]f(s)\,ds,\quad a<x<b, \tag{A1}$$

$$K_1(x,y,s)=\int_0^\infty 4\left(\frac{(-(yb+1)e^{4b\zeta}+((y-2c)b+1)e^{2b\zeta})e^{-y\zeta}}{p(e^{2b\zeta}-1)^2}\right.$$
$$\left.+\frac{(((y-2c)\beta-1)e^{2\beta c}+1-y\beta)e^{y\beta}}{\pi(e^{2\beta c}-1)^2}\right)\beta\cos(\beta(s-x))\,d\beta, \tag{A2}$$

$$K_2(x,y,s)=\sum_{n=1}^{\infty}\frac{2((E_{1n}+E_{2n})e^{-y n\pi/c})+(E_{3n}+E_{4n})e^{y n\pi/c})\pi n\cos\left(\frac{yn\pi}{c}\right)}{E_{5n}c^3}, \tag{A3}$$

where $E_{1n},\ldots,E_{5n}$ are known functions of x and s (see Schulze, 1995). In order to solve the integral eqn (A1) the singular behavior of the kernels K_1 and K_2 must be examined and their principal parts must be separated. This may be done by examining the asymptotic nature of the integrand in (A2) for $\beta\to\infty$ and the terms in (A3) for $n\to\infty$. Thus, for small values of $(s-x)$ and for $\beta\to\infty$, the asymptotic value of K_1 is found to be

$$K_{1a}(x,y,s)=\frac{1}{\pi}\int_0^\infty -(4\beta+4\beta^2 y)e^{-y\beta}\cos(\beta(s-x))\,d\beta$$
$$=-\frac{4}{\pi}\left(\frac{y^2-(s-x)^2}{(y^2+(x-s)^2)^2}+\frac{2y^2(y^2-3(s-x)^2)}{(y^2+(s-x)^2)^3}\right). \tag{A4}$$

Taking the limit $y\to 0$, from (A4) it follows that

$$\lim_{y\to 0}K_{1a}(x,y,s)=\frac{4}{\pi}\frac{1}{(s-x)^2}. \tag{A5}$$

Similarly, for $n\to\infty$ and $(s+x)\to 0$ (i.e., as the crack tip approaches the free surface) from (A3) the asymptotic value of K_2 may be obtained as (Schulze 1995)

$$K_{2a}(x,y,s)=\sum_{n=1}^{\infty}\frac{4\pi}{c^4}(5c^2-3\pi(x+s)cn+2n^2sx\pi^2)e^{-(x+s)n\pi/c}n\cos\left(\frac{yn\pi}{c}\right). \tag{A6}$$

Also, for $n\to\infty$ and small values of $(2h-s-x)$, that is, as the crack tip approaches the interface, from (A3) we find

$$K_{2b}(x,y,s)=\sum_{n=1}^{\infty}4\pi\left(\frac{(10\mu_1^2\kappa_2-(1-\kappa_2)(\kappa_1-9)\mu_2\mu_1-(9+\kappa_1^2)\mu_2^2)n}{c^2(\mu_1\kappa_2+\mu_2)(\mu_1+\kappa_1\mu_2)}-\frac{3\pi(s+x-2h)(\mu_2-\mu_1)n^2}{c^3(\mu_1+\kappa_1\mu_2)}\right.$$
$$\left.-\frac{2\pi^2(s-h)(x-h)(\mu_2-\mu_1)n^3}{c^4(\mu_1+\kappa_1\mu_2)}\right)e^{-n\pi(2h-x-s)/c}\cos\left(\frac{yn\pi}{c}\right). \quad \text{(A7)}$$

If we now sum the series and take the limit $y\to 0$, from (A6) and (A7) we obtain

$$\lim_{y\to 0}K_{2a}(x,y,s)=k_1(x,s)=\frac{4\pi}{c^4}[5c^2F_1(\theta_1)-3\pi(s+x)cF_2(\theta_1)+2\pi^2sxF_3(\theta_1)], \quad \text{(A8)}$$

$$\lim_{y\to 0}K_{2b}(x,y,s)=k_2(x,s)=4\pi\left(\frac{(10\mu_1^2\kappa_2-(1-\kappa_2)(\kappa_1-9)\mu_2\mu_1-(9+\kappa_1^2)\mu_2^2)F_1(\theta_2)}{c^2(\mu_1\kappa_2+\mu_2)(\mu_1+\kappa_1\mu_2)}\right.$$
$$\left.-\frac{3\pi(s+x-2h)(\mu_2-\mu_1)F_2(\theta_2)}{c^3(\mu_1+\kappa_1\mu_2)}-\frac{2\pi^2(s-h)(x-h)(\mu_2-\mu_1)F_3(\theta_2)}{c^4(\mu_1+\kappa_1\mu_2)}\right), \quad \text{(A9)}$$

where

$$F_1(\theta)=\frac{1}{2(\cosh\theta-1)},\quad F_2(\theta)=\frac{\sinh\theta}{2(\cosh\theta-1)^2},\quad F_3(\theta)=\frac{\cosh\theta+2}{2(\cosh\theta-1)^2},$$
$$\theta_1=\frac{\pi}{c}(s+x),\quad \theta_2=\frac{\pi}{c}(2h-s-x). \quad \text{(A10)}$$

Note that the leading terms in the singular kernels k_1 and k_2 defined by (A8) and (A9) may further be separated giving the following more familiar expressions

$$k_1(x,s)=\frac{4}{\pi}k_{1s}(x,s)+k_{1f}(x,s),$$
$$k_{1s}(x,s)=-\frac{1}{(s+x)^2}+\frac{12x}{(s+x)^3}-\frac{12x^3}{(s+x)^4}, \quad \text{(A11)}$$
$$k_2(x,s)=\frac{4}{\pi}k_{2s}(x,s)+k_{2f}(x,s),$$
$$k_{2s}(x,s)=\frac{m_1+12m_2}{2(X+S)^2}-\frac{12m_2X}{(X+S)^3}+\frac{12m_2X^2}{(X+S)^4}, \quad \text{(A12)}$$
$$X=h-x,\quad S=h-s,m_1=\frac{10\mu_1^2\kappa_2-(1-\kappa_2)(\kappa_1-9)\mu_1\mu_2-(9+\kappa_1^2)\mu_2^2}{(\mu_1\kappa_2+\mu_2)(\mu_1+\mu_2\kappa_1)}, \quad \text{(A13)}$$
$$m_2=\frac{\mu_2-\mu_1}{\mu_1+\mu_2\kappa_1}, \quad \text{(A14)}$$

where k_{1s} and k_{2s} are the standard generalized singular kernels that become unbounded as x and s approach the free boundary $x=0$ and the interface $x=h$, respectively, and k_{1f} and k_{2f} are bounded in the closed interval $0\leqslant(x,s)\leqslant h$. Finally, we observe that the integral eqn (A1) may be expressed as

$$\frac{1}{\pi}\int_a^b\left[\frac{1}{(s-x)^2}+k_{1s}(x,s)+k_{2s}(x,s)+k_f(x,s)\right]f(s)\,ds=\frac{\kappa_1+1}{4m_1}p(x),a<x<b, \quad \text{(A15)}$$

where the known function k_f is square-integrable in $0\leqslant(x,s)\leqslant h$.